J. Membrane Biol. 112, 277–289 (1989)

The Journal of
Membrane Biology


# Temperature Dependence of Gating Current in Myelinated Nerve Fibers

Peter Jonas
Physiologisches Institut der Justus-Liebig-Universität Giessen, D-6300 Giessen, Federal Republic of Germany

**Summary.** Asymmetrical displacement currents and Na currents of single myelinated nerve fibers of *Xenopus laevis* were studied in the temperature range from 5 to 24°C. The time constant of the on-response at $E = 4$ mV, $\tau_{on}$, was strongly temperature dependent, whereas the amount of displaced charge at $E = 39$ mV, $Q_{on}$, was only slightly temperature dependent. The mean $Q_{10}$ for $\tau_{on}^{-1}$ was 2.54, the mean $Q_{10}$ for $Q_{on}$ was 1.07. The time constant of charge immobilization, $\tau_i$, at $E = 4$ mV varied significantly ($\alpha = 0.001$) with temperature. The mean $Q_{10}$ for $\tau_i^{-1}$ was 2.71 ± 0.38. The time constants of immobilization of gating charge and of fast inactivation of Na permeability were similar in the temperature range from 6 to 22°C. The $Q_{off}/Q_{on}$ ratio for $E = 4$ mV pulses of 0.5 msec duration decreased with increasing temperature. The temperature dependence of the time constant of the off-response could not be described by a single $Q_{10}$ value, since the $Q_{10}$ depended on the duration of the test pulse. Increasing temperature shifted $Q_{on}$ $(E)$ curves to more negative potentials by 0.51 mV $K^{-1}$, but shifted $P_{Na}$ $(E)$ curves and $h_\infty$ $(E)$ curves to more positive potentials by 0.43 and 0.57 mV $K^{-1}$, respectively. $h_\infty$ ($E = -70$ mV) increased monotonously with increasing temperature. The present data indicate that considerable entropy changes may occur when the Na channel molecule passes from closed through open to inactivated states.

**Key Words** myelinated nerve fiber · gating current · temperature

## Introduction

Since the first measurement on nerve membrane by Armstrong and Bezanilla (1973), asymmetry currents have been demonstrated to be, at least mostly, associated with the opening and closing of Na channels. Therefore, it seems to be justified to use the terms "asymmetry current" and "gating current" synonymously. The relation between activation of macroscopic current and charge movement, on one hand, and between inactivation of macroscopic current and charge immobilization, on the other hand, may be rather complex. Gating current reflects mainly reaction steps before, but also after the one that opens the Na channel (Neumcke, Nonner & Stämpfli, 1976). The role of charge immobilization remains unclear. Armstrong and Bezanilla (1977) reported that kinetics and potential dependence of immobilization and inactivation are similar, whereas Meves and Vogel (1977) found that immobilization develops four times slower than inactivation. Nonner (1979) reported that both processes are similarly affected by a scorpion venom, whereas Tanguy and Yeh (1988) observed that batrachotoxin removes inactivation but enhances charge immobilization. Thus, it is most likely that charge immobilization and inactivation are linked, but reflect different molecular steps (Nonner, 1980).

The effect of temperature on gating current was first investigated by Bezanilla and Taylor (1978) and Kimura and Meves (1979) on squid axon. The temperature dependence of charge immobilization has not been characterized yet. Whereas it is accepted that steady-state parameters of Na permeability are shifted when temperature is changed (Dudel & Rüdel, 1970; Kimura & Meves, 1979; Chiu, Mrose & Ritchie, 1979; Schwarz, 1986), little has been known about how stationary gating current parameters change with temperature. Altogether, only two short reports deal with the influence of temperature on gating current in amphibian nerve fibers (Nonner, Rojas & Stämpfli, 1975; Collins & Rojas, 1982). The aim of the present study was to measure temperature dependence of gating current and Na current of the node of Ranvier under similar conditions and to integrate these data into a thermodynamic model of Na channel gating. Previous findings on squid axon are extended in regard to temperature dependence of charge immobilization and steady-state parameters. It is concluded that considerable entropy changes may be associated with conformational changes of the Na channel protein. A preliminary account of some of the experiments has been published elsewhere (Jonas & Vogel, 1988).

## Materials and Methods

Single myelinated nerve fibers were dissected from the motor or sensory branch of the tibial nerve of decapitated clawed toads (*Xenopus laevis*). The fibers were mounted in a Perspex chamber, fixed with Vaseline or Glisseal (Borer Chemie, Solothurn, Switzerland) seals, and held under current or voltage-clamp conditions (Nonner, 1969). Both ends of the fiber were cut as short as possible in order to increase the bandwidth of the recordings (Nonner, Rojas & Stämpfli, 1978). The absolute membrane potential, where $h_\infty$was 0.6–0.8 at about 12°C, was assumed to be $E = -70$ mV and the holding potential was adjusted to $E = -100$ mV throughout the experiment. The preparation was allowed to stabilize before the measurement began. Membrane current values, $I_m$, were calculated from the voltages at the compartment $E$ as $I_m = V_E/R_{ED}$, where $R_{ED}$, the axoplasmic resistance between compartment $E$ and the node, was estimated from the actual fiber geometry and a specific axoplasmic resistance of 100 Ω cm. The decrease of $R_{ED}$ with increasing temperature with a $Q_{10}$ of 1.22 (Neumcke & Stämpfli, cited in Schwarz, 1986) or about 1.3 (Chiu et al., 1979) was not taken into account. The current signals were filtered by a 4-pole low-pass Bessel filter with corner frequencies of 20 or 28 kHz (3 dB attenuation).

The temperature of the preparation was measured with a thermocouple in the nodal compartment A less than 2 mm distant from the node and was continuously recorded with a multi-pen recorder. The accuracy of this kind of temperature measurement was estimated to be about ±0.3°C. Two Peltier elements cooled or heated the aluminium block surrounding the nerve chamber and the solution flowing through the nodal compartment. The temperature was changed slowly (by about 1°C $min^{-1}$) to avoid hysteresis effects (*see* Schwarz, 1979).

A Sirius 1 microcomputer (Sirius Systems Technology, Scotts Valley, CA 95066) generated pulses via a 12-bit digital-to-analog converter and sampled membrane currents via a 12-bit analog-to-digital converter at a rate of a multiple of 5 μsec (de Haas, 1987). Gating currents and Na currents were elicited with the same pulse program. It consisted of a 50-msec prepulse with $E = -120$ mV, a test pulse with $E = E_{test}$ of 0.25 to 30 msec duration and a 2-msec postpulse with $E = -120$ mV. For measurement of gating currents, most of the leakage and capacity current was subtracted analogically and the residual symmetrical current was subtracted digitally by means of a +P/2 procedure, i.e., with two voltage jumps from $E = (-120\text{ mV} - \Delta E/2)$ to $E = -120$ mV, where $\Delta E = E_{test} - (-120\text{ mV})$. For measurement of Na currents, leakage and capacity currents were estimated from a negative pulse and subtracted digitally. Usually, 1 to 16 (Na currents) and 32 and 448 (asymmetry currents) single sweeps were averaged to improve the signal-to-noise ratio. The interpulse interval was chosen long enough (0.9 sec) to allow sufficient recovery from inactivation. Charge *vs.* voltage curves, $Q_{on}(E)$, were obtained from two runs, one with increasing pulse potential and the other one with decreasing pulse potential; corresponding records were finally averaged. This procedure was chosen to avoid systematical errors, which could arise if, for instance, $Q_{on}$ values at lower potentials are always measured before the $Q_{on}$ values at higher potentials. Similarly, immobilization curves were obtained from one run with increasing pulse length and another run with decreasing pulse length. The error of charge due to the recording apparatus, $Q_{app}$, was determined with a realistic dummy circuit representing the nerve fiber and the seal resistances (membrane capacity $C_m = 8.2$ pF, series resistance $R_s = 1.0$ MΩ, $R_{ED} = 3.3$ MΩ). $Q_{app}$ was estimated to be 4.2 fC for the on-charge moving during a 0.5-msec pulse with $E =$ 4 mV. Compared to the gating current of the Na channels (*see* results), this is about two orders of magnitude smaller.

In order to take the delay of the current signal introduced by the low-pass filter into account, the time axis of the current recordings was shifted by 15 μsec with respect to that of the pulses (Nonner et al., 1978). Time constants $\tau$ of the on- and off-responses of the asymmetry current were obtained after integration and fit with the function

$$Q(t) = Q_\infty \cdot [1\text{-}\exp(-t/\tau)] + I \cdot t. \quad (1)$$

The linear term $I \cdot t$ allows for very slow components of charge movement (e.g., off-response components due to the return of immobilized charge) or components of constant current (e.g., the "pedestal" of on-responses). Usually, only data points with 0.02 msec $\leq t \leq$ 1 msec for the on-responses and 0.02 msec $\leq t \leq 0.3$ msec for the off-responses were taken into account. The amount of displaced charge was either obtained from fit with Eq. (1) or by integration for $0 \leq t \leq 0.5$ msec. The last method required the subtraction of the pedestal, which was measured between 0.5 and 1 msec after the onset of the pulse. Displaced charge is always given as a positive value regardless of the direction of the current flow.

Time constants of activation and inactivation of Na permeability were obtained from fit with the function

$$I_{Na}(t) = \begin{cases} \{1 - \exp[-(t - \delta t)/\tau_m]\}^2 \cdot [A \cdot \exp(-t/\tau_h) \\ \quad + B] \text{ for } t \geq \delta t \\ 0 \text{ for } t < \delta t \end{cases} \quad (2)$$

(*see* Neumcke et al., 1976). Usually, only data points with 0.02 msec $\leq t \leq 5$ msec were taken into account. Instead of a slow exponential component of inactivation (Kniffki, Siemen & Vogel, 1981), a time-independent component $B$ was introduced. This simplification accelerated the convergence of the fit algorithm remarkably. The $\tau_h$ values obtained with Eq. (2) are nearly equal to the $\tau_{h1}$ values of Kniffki et al. (1981; *compare* their Fig. 3 with Fig. 4*B* of the present paper).

$Q_{on}(E)$ curves, $P_{Na}(E)$ curves, and $h_\infty(E)$ curves (*see* Fig. 6) were fitted with the function

$$Y(E) = Y_{max}/\{1 + \exp[(E_h - E)/k^*]\},\ Y = Q_{on},\ P_{Na},\text{ or } h_\infty, \quad (3)$$

where $E_h$ is the midpoint potential of the curve and $k^*$ is the slope factor. $Y_{max}$ was set to 1 for $Y = h_\infty$.

Nonlinear least squares fits were performed by means of an improved Gauss-Newton method (Jennrich & Ralston, 1979), which also provided the standard error of each estimated parameter. Mean values (e.g., in Tables 1 and 2) are given as mean ± SEM unless otherwise noted. In some plots (Figs. 4 and 7), points within a ± 0.5°C temperature interval are condensed to one mean value in order to increase the clarity of the illustrations. Error bars indicate the SEM if it exceeds the size of the symbol. The statistical significance of a correlation between two parameters was estimated from the value of the correlation coefficient according to Sachs (1984).

During the measurement of asymmetry currents, the node was continuously superfused with a standard solution containing (in mM) 107 tris(hydroxymethyl)-aminomethane (Tris) chloride, 2.0 $CaCl_2$, 10 tetraethylammoniumchloride (TEA), and 500 nM tetrodotoxin (TTX), pH = 7.4 ± 0.05. In some experiments, 97 mM tetramethylammoniumchloride and 10 mM TrisCl were used instead of 107 mM TrisCl. During the measurement of Na currents, the fiber was superfused with a Ri-TEA solution contain-

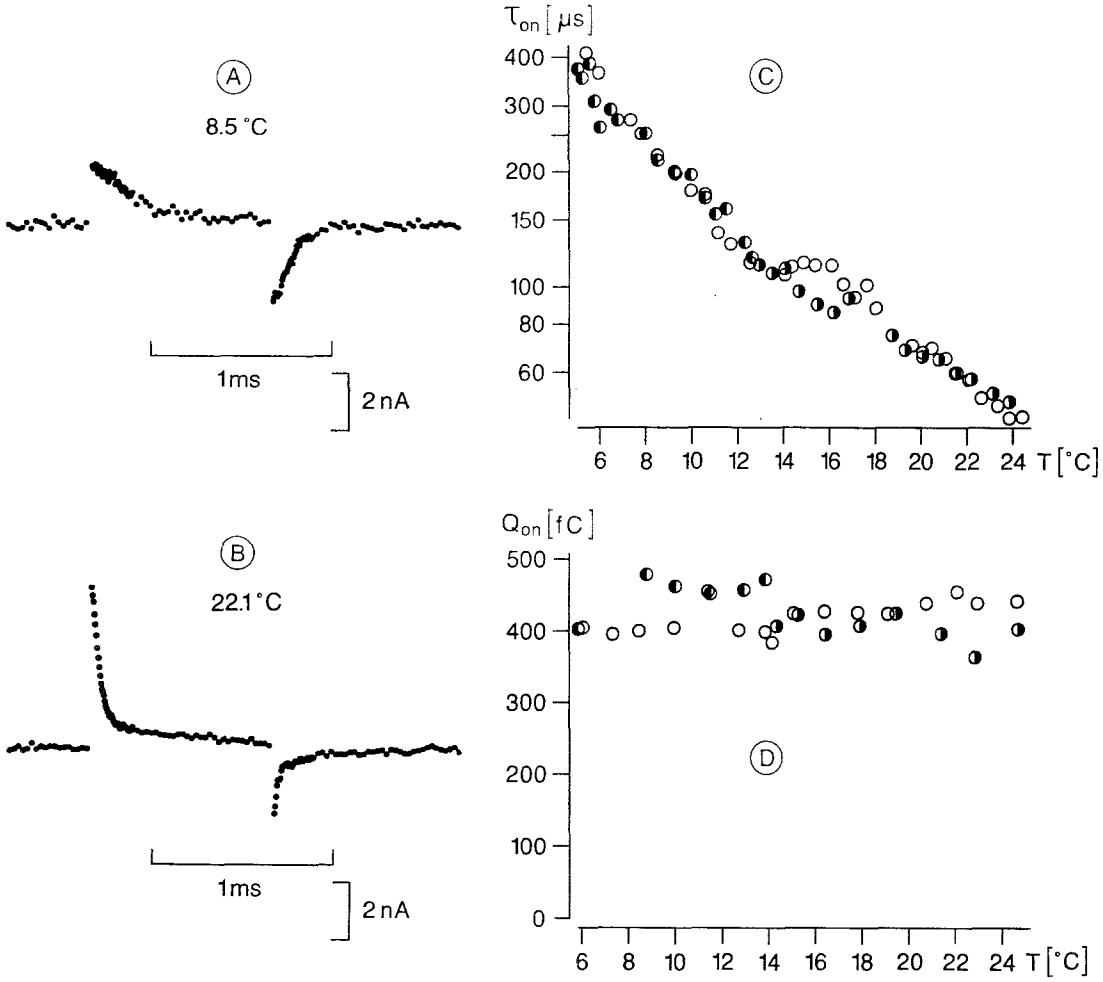


**Fig. 1.** Temperature dependence of asymmetry current kinetics and amount of displaced charge. (*A*, *B*) Original recordings are shown of asymmetry currents at 8.5°C (*A*) and 22.1°C (*B*). Current responses to 32 pulses were averaged. The first five sample points after each voltage step, corresponding to 25 μsec, are not plotted. Corner frequency of the low-pass filter was 28 kHz; test pulse $E = 4$ mV. (*C*) Time constant of the on-response of the asymmetry current, $\tau_{on}$, was plotted logarithmically *vs.* temperature. $\tau_{on}$ was obtained from fit with Eq. (1). Test pulse $E = 4$ mV. (*D*) Amount of displaced charge, $Q_{on}$, was plotted *vs.* temperature. $Q_{on}$ was obtained from direct integration of the first 0.5 msec of the on-response after subtraction of the pedestal (0.5–1 msec). Test pulse $E = 39$ mV. Data in *C* and *D* are from one temperature cycle each; the sequence of measurements was: from intermediate to low (◐), from low to high (○), and from high to intermediate temperature (◑). Expt. TE805

ing (in mM) 110 NaCl, 2.5 KCl, 2.0 $CaCl_2$, 5.0 N,N-bis(2-hydroxyethyl)-2-aminoethane sulfonic acid (BES), 10 TEA, pH adjusted to 7.4 ± 0.05 with Tris base. TTX (5 nM) was added in most of the Na current experiments to minimize artifacts due to series resistance, $R_s$. $R_s$ could pretend shifts of $P_{Na}(E)$ curves, because the peak current increases with temperature. The precise estimation of the amount of shift due to $R_s$ is, however, difficult, because $R_s$ may be temperature dependent itself. Assuming the most unfavorable case of a temperature-independent $R_s = 280$ kΩ (Drouin & Neumcke, 1974), $P_{Na} = 3 \times 10^{-9}$ cm³ sec⁻¹ (25°C), $P_{Na} = 1.5 \times 10^{-9}$ cm³ sec⁻¹ (5°C), a reversal potential $E_{Na} = 60$ mV, and $E_h = -40$ mV (*see* Fig. 6*B*), one can calculate a $P_{Na}$ shift of 4 mV to the left when temperature is increased. The cut ends of the fiber were bathed in a solution containing, in mM, 110 CsF, 10 TrisCl, pH = 7.2 ± 0.05. Control measurements revealed that electrode potentials and junction potentials are constant within about ±1 mV when temperature is changed from 5 to 25°C.

## Results

### Temperature Dependence of $\tau_{on}$ and $Q_{on}$

Figure 1*A* and *B* show asymmetry currents recorded at 8.5°C and 22.1°C. The test pulse potential was $E = 4$ mV, the potential before and after the testpulse was $E = -120$ mV. The kinetics of on-response and off-response of the asymmetry current are both faster at 22.1°C as compared with 8.5°C. Although the maximum asymmetry current is higher at higher temperature, the amount of charge $Q_{on}$ carried during the first 0.5 msec of the on-response after subtraction of the pedestal is similar in both cases ($Q_{on} = 414$ fC at 8.5°C, $Q_{on} = 423$ fC at 22.1°C).

**Table 1.** Temperature dependence of $Q_{on}$

| Expt. | $Q_{10}$ | Temperature range (°C) | Significant correlation[a] |
|---|---|---|---|
| AS724 | 1.06 | 5.6–21.2 | yes |
| AS726 | 1.11 | 6.2–19.1 | no |
| AS727 | 1.27 | 4.3–21.1 | yes |
| AS730 | 0.92 | 8.2–18.7 | no |
| TE805 | 0.99 | 5.9–24.7 | no |
| Mean ± SEM | 1.07 ±0.06 | | |

[a] Two-sided test, $\alpha = 0.05$.

The effect of temperature on the kinetics of the on-response is quantitatively analyzed in Fig. 1*C*. The time constant of the on-response, $\tau_{on}$, was obtained by fitting integrated on-responses with Eq. (1) and was plotted logarithmically *vs.* temperature. For $t \leq 1$ msec, the time course of the on-responses could be sufficiently described by one exponential function and a linear term (correlation coefficient, $r$, between 0.9999 and 0.9913). At temperatures above 20°C, a second slower component was sometimes visible, but was not analyzed further. The mean $Q_{10}$ value for $\tau_{on}^{-1}$ obtained from eight experiments was 2.54 ± 0.07 (*see* legend of Fig. 7) in the temperature range 5–24°C.

In Fig. 1*D*, the amount of charge $Q_{on}$ carried during the first 0.5 msec of a test pulse with $E = 39$ mV was plotted *vs.* temperature. The high test-pulse potential was chosen to give an estimate of the maximum amount of displaced charge. Qualitatively, $Q_{on}$ does not increase with temperature; it even decreases slightly in this experiment. Table 1 lists the $Q_{10}$ values for $Q_{on}$ obtained from five experiments. A significant variation of $Q_{on}$ with temperature was only seen in two of these experiments. The mean $Q_{10}$ value for $Q_{on}$ at $E = 39$ mV is 1.07 ± 0.06.

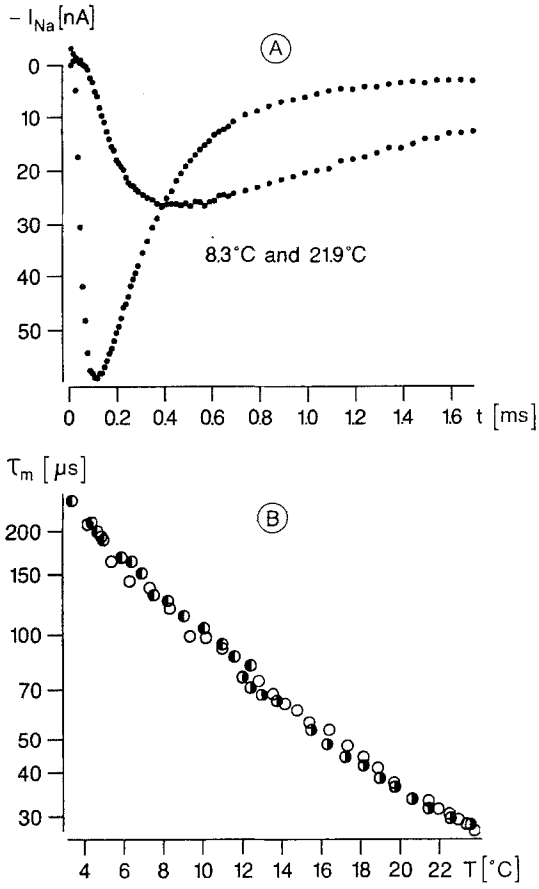


**Fig. 2.** Temperature dependence of Na current kinetics. (*A*) Na currents are shown at 8.3 and 21.9°C in Ri-TEA + 5 μM TTX. The registration with the larger peak current was recorded at higher temperature. Current responses to 16 pulses were averaged. Corner frequency of the low-pass filter was 28 kHz (Expt. TE802). (*B*) Time constant of Na permeability activation, $\tau_m$, is shown plotted logarithmically *vs.* temperature. $\tau_m$ was obtained from fit with Eq. (2). Data are from one temperature cycle; the different symbols have the same meaning as in Fig. 1 (Expt. TE804). Test pulse $E = 4$ mV throughout the figure

## Temperature Dependence of $\tau_m$

Frankenhaeuser and Moore (1963) reported surprisingly low $Q_{10}$ values for the activation kinetics of Na permeability. It therefore seemed interesting to reinvestigate this point with improved techniques of data acquisition and evaluation. Figure 2*A* shows recordings of Na currents at 8.3 and 21.9°C. TTX (5 nM) was added to the extracellular solution in order to reduce series resistance artifacts. The Na current recordings of Fig. 2*A* may be compared with the gating current recordings of Fig. 1*A* and *B*, because prepulse potential (−120 mV), testpulse potential (4 mV), internal solution, and temperature are similar. The kinetics of activation and inactivation is faster and the peak current is larger at 21.9 than at 8.3°C. The time constant, $\tau_m$, of the Na permeability activation was plotted logarithmically *vs.* temperature in Fig. 2*B*. $\tau_m$ values were obtained by fitting Na current recordings with Eq. (2), which includes an exponent of two and an additional delay term (Neumcke et al., 1976). The mean $Q_{10}$ value for $\tau_m^{-1}$ obtained from five experiments was 2.64 ± 0.06 (*see* legend of Fig. 7) in the temperature range 5–24°C.

The present data indicate that the $Q_{10}$ values for $\tau_{on}^{-1}$ of the gating current and the $Q_{10}$ values for $\tau_m^{-1}$ of the Na current are not significantly different. Figures 1*C* and 2*B* present data obtained from one cyclic change of temperature each. Since the $\tau$ value at the beginning of the temperature cycle is equal to

the $\tau$ value at the end of the temperature cycle, the effects of temperature on $\tau_{on}$ and $\tau_m$ seem to be fully reversible. The $Q_{10}$ value for $\tau_{on}^{-1}$ and $\tau_m^{-1}$ is slightly larger at low temperature than at high temperature. A slight temperature dependence of the $Q_{10}$ value is, however, expected even if activation enthalpy is constant (*see* Kniffki et al., 1981). There is no evidence for a phase transition in the temperature range 5–24°C (Schwarz, 1979).

## Temperature Dependence of Charge Immobilization

Figure 3 shows the temperature dependence of charge immobilization kinetics. $Q_{off}/Q_{on}$ is plotted *vs.* the length of the immobilizing pulse ($E$ = 4 mV) at 5.8 and 6.2°C in Fig. 3*A* and at 18.9°C in Fig. 3*B*. Charge immobilization develops faster at higher temperature. The points can be satisfactorily fitted with one exponential function and a component of nonimmobilizable charge $Q_n$ (*see* legend of Fig. 3). $Q_n/(Q_i + Q_n)$ was slightly higher at higher temperature, but its temperature dependence was not significant ($r$ = 0.52, 12 degrees of freedom, two-sided test, $\alpha$ = 0.05). $Q_n/(Q_i + Q_n)$ estimated from 14 immobilization curves at various temperatures is 21.6 ± 8.25% (mean value ± SD, eight fibers). If charge immobilization has a temperature-dependent kinetics, one would expect that the $Q_{off}/Q_{on}$ ratio for pulses of constant length varies with temperature. Figure 3*C* shows that this is the case. The $Q_{off}/Q_{on}$ ratio for 0.5-msec pulses decreases monotonously from values of about 0.8 at 6°C to values of approximately 0.4 at 22°C.

Figure 4*A* shows the time constant of charge immobilization, $\tau_i$, plotted logarithmically *vs.* temperature. $\tau_i$ values were obtained with two different methods: (i) $Q_{off}/Q_{on}(t_{pulse})$ was fitted with an exponential function as shown in Fig. 3*A* and *B*. (ii) Alternatively, $\tau_i$ was obtained from the $Q_{off}/Q_{on}$ ratio for a pulse of constant length (*see* Fig. 3*C*): If $Q_{off}/Q_{on}(t_{pulse}) = Q_i \cdot \exp(-t_{pulse}/\tau_i) + Q_n$ and if one assumes that $Q_i$ and $Q_n$ do not change with temperature, it follows that

$$\tau_i = -t_{pulse}/\ln[(Q_{off}/Q_{on} - Q_n)/Q_i]. \quad (4)$$

Hence, $\tau_i$ can be directly obtained from the $Q_{off}/Q_{on}$ ratio if $Q_i$ and $Q_n$ are determined once in each experiment. Method *i* allows a more precise estimation of $\tau_i$, but it is not possible to measure $\tau_i$ at more than two or three temperatures in one fiber. Method *ii* makes it possible to determine $\tau_i$ for a lot of temperatures in one fiber, but produces considerable scatter of data, because each $\tau_i$ depends on only one $Q_{off}/Q_{on}$ value. It may lead to incorrect results if $Q_i$

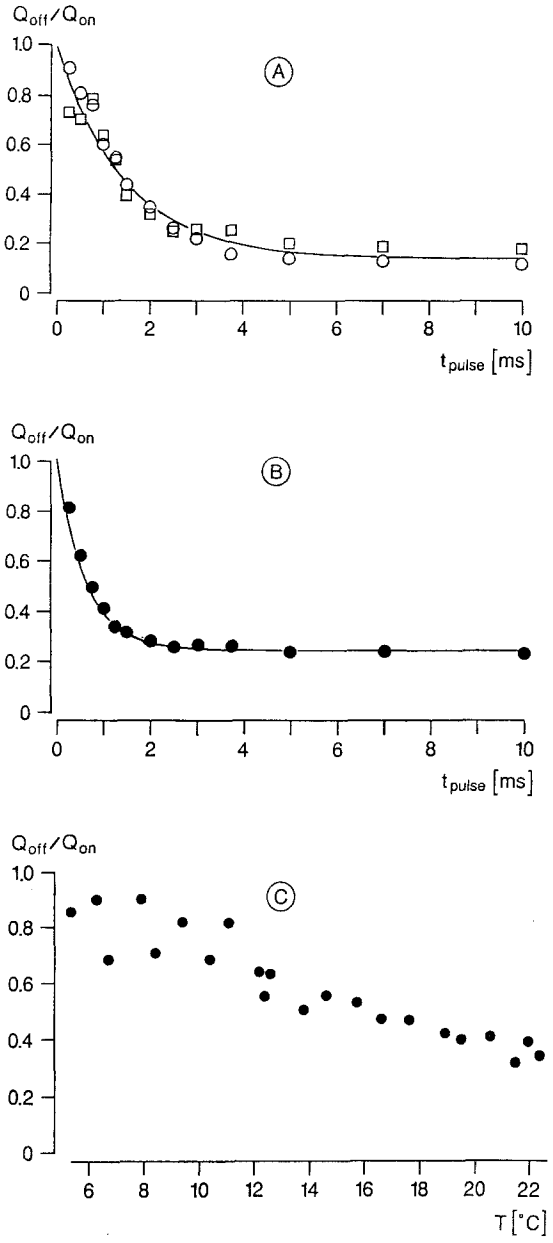


**Fig. 3.** Temperature dependence of charge immobilization kinetics. (*A*) Relative off-response charge, $Q_{off}/Q_{on}$, is shown plotted *vs.* pulse length, $t_{pulse}$, at 6.2°C (○) and 5.8°C (□), (*B*) at 18.9°C (●). $Q_{off}(t_{pulse})$ was obtained by fitting the off-response (0.3 msec) after pulses of duration $t_{pulse}$ with Eq. (1). $Q_{on}(t_{pulse})$ was obtained by averaging all corresponding on-responses and fitting them with Eq. (1). The continuous curves are drawn according to least squares fits with the function $Q_{off}/Q_{on}(t_{pulse}) = Q_i \cdot \exp(-t_{pulse}/\tau_i) + Q_n$ to the mean of the points (○) and (□) in *A* and the points (●) in *B*. $\tau_i$ = 1.47 msec and $Q_n$ = 0.138 in *A*, $\tau_i$ = 0.61 msec and $Q_n$ = 0.246 in *B*. Points at $t_{pulse}$ = 15 msec were included into the fit, but are not displayed in the figure. Sequence of the measurements was (A ○), (B ●), (A □) (Expt. AS726). (*C*) $Q_{off}/Q_{on}$ was obtained with test pulses of a constant duration of 0.5 msec. $Q_{off}$ was obtained as in *A* and *B*, but $Q_{on}$ was obtained by direct integration of the on-response, because the pulses are short (Expt. AS740). Immobilizing pulse $E$ = 4 mV throughout the figure

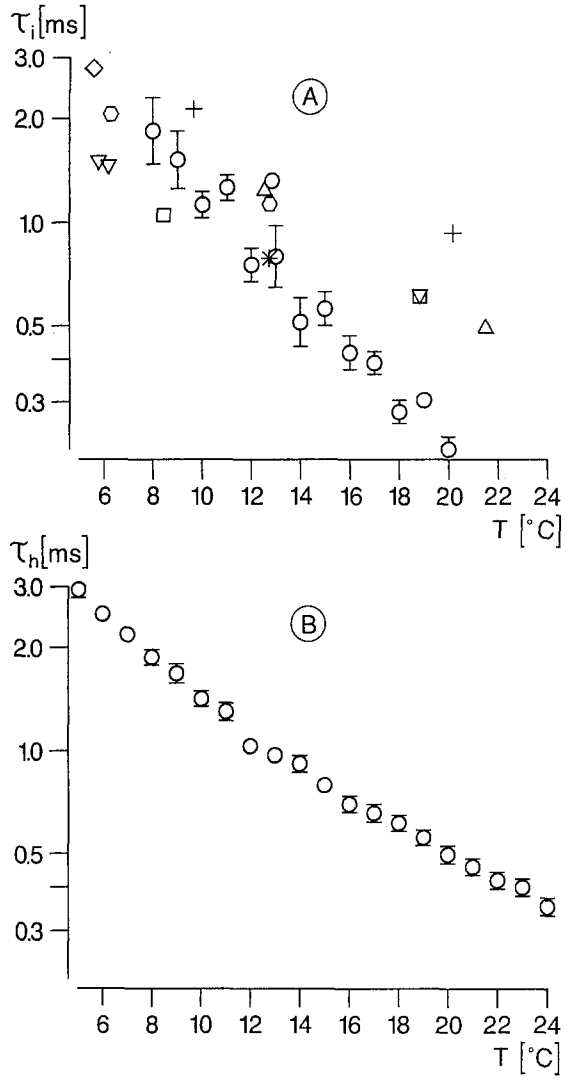


**Fig. 4.** Temperature dependence of immobilization time constant compared with fast inactivation time constant. (*A*) Time constants of charge immobilization, $\tau_i$, are shown plotted logarithmically *vs.* temperature. Circles: $\tau_i$ was obtained from $Q_{off}/Q_{on}$ according to Eq. (4), data from 81 gating current records (two experiments), test-pulse length 0.25, 0.5, 0.75, and 1.0 msec. All other symbols: $\tau_i$ was obtained from fit of $Q_{off}/Q_{on}$ ($t_{pulse}$) as in Fig. 3*A* and *B*, data from eight experiments; different experiments are represented by different symbols. The symbol (▽) corresponds to the experiment of Fig. 3*A*, *B*. Immobilizing pulse $E$ = 4 mV. (*B*) Time constants of fast inactivation of Na permeability, $\tau_h$, are shown plotted logarithmically *vs.* temperature. Data are from 394 Na current records (five experiments). Test pulse E = 4 mV

and $Q_n$ are not temperature independent and if $Q_{off}/Q_{on}(t_{pulse})$ is not sufficiently described by a single exponential term. A slight temperature dependence of $Q_n$ indeed cannot be excluded (*see* above). In Fig. 4*A*, the circles represent mean $\tau_i$ values obtained with method *ii*, all other symbols represent data obtained with method *i*. The mean $Q_{10}$ value for $\tau_i^{-1}$ is 2.71 ± 0.38 if the $\tau_i$ values obtained with method *i* are weighted with a factor of 2 because of their higher reliability. The correlation between $\tau_i$ and temperature is highly significant ($r = -0.81$, 25 degrees of freedom, two-sided test, $\alpha = 0.001$). For comparison, Fig. 4*B* shows the time constant of Na permeability inactivation, $\tau_h$, plotted logarithmically *vs.* temperature. $\tau_h$ was obtained from fit of Na currents with Eq. (2). The mean $Q_{10}$ value for $\tau_h^{-1}$ is 3.00 ± 0.09 (*see* legend of Fig. 7). Thus, the $Q_{10}$ values for $\tau_i^{-1}$ and $\tau_h^{-1}$ are not significantly different. Moreover, $\tau_i$ and $\tau_h$ are similar within the investigated temperature range 6–22°C.

### Temperature Dependence of $\tau_{off}$

Figure 5*A* and *B* shows integrated off-responses after a voltage jump from $E$ = 4 mV to $E$ = −120 mV at 6.2 and 18.9°C. The duration of the test pulses was 0.25, 0.75, 1.5 and 2.5 msec. The kinetics of the off-response is faster at higher temperature. Figure 5*C* displays the time constants of the off-response at 6.2 and 18.9°C obtained from fit with Eq. (1). At low temperature, $\tau_{off}$ increases with increasing test-pulse duration, reaches a maximum value at 0.75 msec, and then decreases again. At high temperature, the rising phase is less pronounced. A similar dependence of $\tau_{off}$ on pulse length was reported by Dubois and Schneider (1982). The authors suggested that $\tau_{off}$ increases with increasing amount of $Q_{on}$ and decreases as charge immobilization develops. Figure 5*C* shows clearly that the determination of the $Q_{10}$ value for $\tau_{off}^{-1}$ with pulses of a constant duration may give different values, depending on the length of the pulse. 0.25-msec pulses yield a $Q_{10}$ of only 1.74, whereas 1.5-msec pulses give a $Q_{10}$ of 2.52. Such a dependence of $Q_{10}$ on pulse duration is in accordance with the suggestions of Dubois and Schneider (1982), since the maximum of $\tau_{off}(t_{pulse})$ would be shifted towards lower $t_{pulse}$ values when on-response kinetics and immobilization kinetics become faster as temperature is increased.

### Temperature Dependence of $Q_{on}(E)$, $P_{Na}(E)$, and $h_\infty(E)$

Figure 6*A–C* shows the effect of temperature on stationary gating parameters as functions of potential. The filled circles represent measurements at about 25°C; the open circles symbolize measurements at approximately 5°C. The half-filled symbols represent the average from three measurements at about 13°C, which have been performed before, between, and after the measurements at 5 and 25°C.

In Fig. 6*A*, the on-response charge, $Q_{on}$, was plotted *vs.* test-pulse potential $E$ for different temperatures. $Q_{on}(E)$ was fitted with Eq. (3) and all $Q_{on}$ values were normalized to the maximum charge ($Y_{max}$ in Eq. (3)). Increasing temperature by 18.6°C shifts $Q_{on}(E)$ curves towards negative potentials by

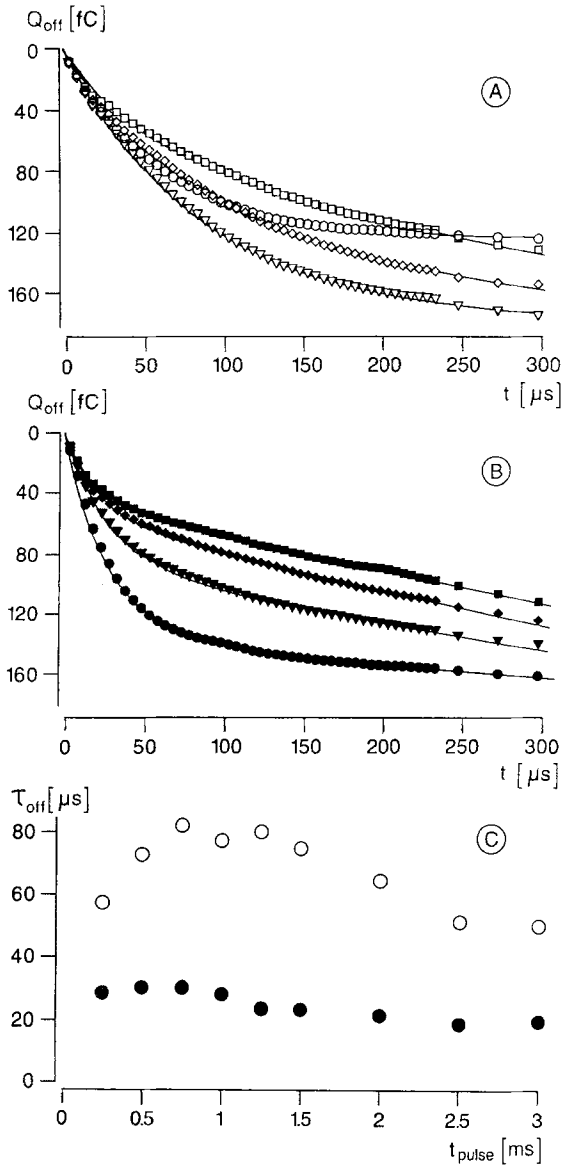


**Fig. 5.** Temperature dependence of $\tau_{off}$. (*A*, *B*) Integrated off-responses of asymmetry currents are shown at 6.2°C (*A*) and 18.9°C (*B*). Length of the immobilizing pulse: $t_{pulse}$ = 0.25 msec (circles), 0.75 msec (triangles), 1.5 msec (diamonds), and 2.5 msec (squares). Zero-current line was estimated from 39 samples (1 msec) directly before the onset of the test pulse and 39 samples (1 msec) 1 msec after the end of the test pulse. The continuous curves were obtained from fit with Eq. (1). (*C*) Time constant of the integrated off-responses, $\tau_{off}$, was plotted *vs.* length of the immobilizing pulse, $t_{pulse}$, at 6.2°C (○) and 18.9°C (●). Potential of the immobilizing pulse $E$ = 4 mV, potential after the pulse $E$ = −120 mV. (Expt. AS726)

11.8 mV. The estimation of the midpoint potentials seems to be quite reliable, because the $Q_{on}(E)$ curves at high as well as at low temperature saturate in the positive potential range. In Fig. 6*B*, Na permeability, $P_{Na}$, is plotted logarithmically *vs.* test-pulse potential. Increasing temperature by 20.0°C shifts $P_{Na}(E)$ towards positive potentials by 8.3 mV.

**Table 2.**

A. Temperature dependence of midpoint potential of $Q_{on}(E)$ curves

| Expt. | Shift (mV) | Temperature range (°C) | Slope factor $\|k^*\|$ (mV) low/high temp. |
|---|---|---|---|
| AS719 | −8.3 | 5.6–24.8 | 15.2/22.5 |
| AS724 | −8.6 | 5.6–21.1 | 13.1/15.1 |
| AS726 | −9.2 | 6.0–19.1 | 18.0/22.4 |
| AS734 | −2.6 | 7.4–19.3 | 24.0/20.5 |
| TE805 | −11.8 | 6.1–24.7 | 15.3/18.0 |
| Mean | −0.508 mV $K^{-1}$ | | 18.41 |
| ± SEM | ±0.085 | | ± 1.19 |

B. Temperature dependence of midpoint potential of $P_{Na}(E)$ curves[a]

| Expt. | Shift (mV) | Temperature range (°C) | Slope factor $\|k^*\|$ (mV) low/high temp. |
|---|---|---|---|
| TE804 | 5.2 | 3.9–24.6 | 5.5/4.6 |
| TE806 | 8.3 | 4.3–24.3 | 7.2/5.3 |
| TE810 | 10.2 | 5.6–21.9 | 4.1/3.9 |
| Mean | 0.429 mV $K^{-1}$ | | 5.10 |
| ± SEM | ±0.109 | | ±0.49 |

C. Temperature dependence of midpoint potential of $h_\infty(E)$ curves

| Expt. | Shift (mV) | Temperature range (°C) | Slope factor $\|k^*\|$ (mV) low/high temp. |
|---|---|---|---|
| TE804 | 13.9 | 4.1–25.4 | 7.3/5.5 |
| TE806 | 10.4 | 4.2–24.3 | 8.7/7.2 |
| TE807 | 7.2 | 5.2–23.3 | 8.1/5.8 |
| TE810 | 11.9 | 5.3–22.0 | 9.5/7.8 |
| Mean | 0.570 mV $K^{-1}$ | | 7.49 |
| ± SEM | ±0.070 | | ±0.48 |

[a] Midpoint potentials of the $P_{Na}(E)$ curves were obtained from semilogarithmic plots as in Fig. 6*B*; a logarithmic form of Eq. (3) was used for the fit.

Figure 6*C* shows steady-state inactivation, $h_\infty$, plotted *vs.* prepulse potential. The length of the prepulses was 50 msec for the curve at 25.4°C and 250 msec for the curve at 4.1°C to compensate for the slower inactivation kinetics at lower temperature. The $h_\infty(E)$ curve is shifted towards positive potentials by 13.9 mV when temperature is increased by 21.3°C.

As the 95% confidence intervals of the midpoint potentials do not overlap (*see* legend of Fig. 6), the difference between $E_h$ at low and high temperature is significant for all curves. The shifts seem to occur in the whole temperature range 5–25°C, because the points at intermediate temperature are between the curves at low and high temperature. Shifts of $Q_{on}(E)$, $P_{Na}(E)$, and $h_\infty(E)$ observed in nine experiments including the data of Fig. 6 are summarized in Table 2.

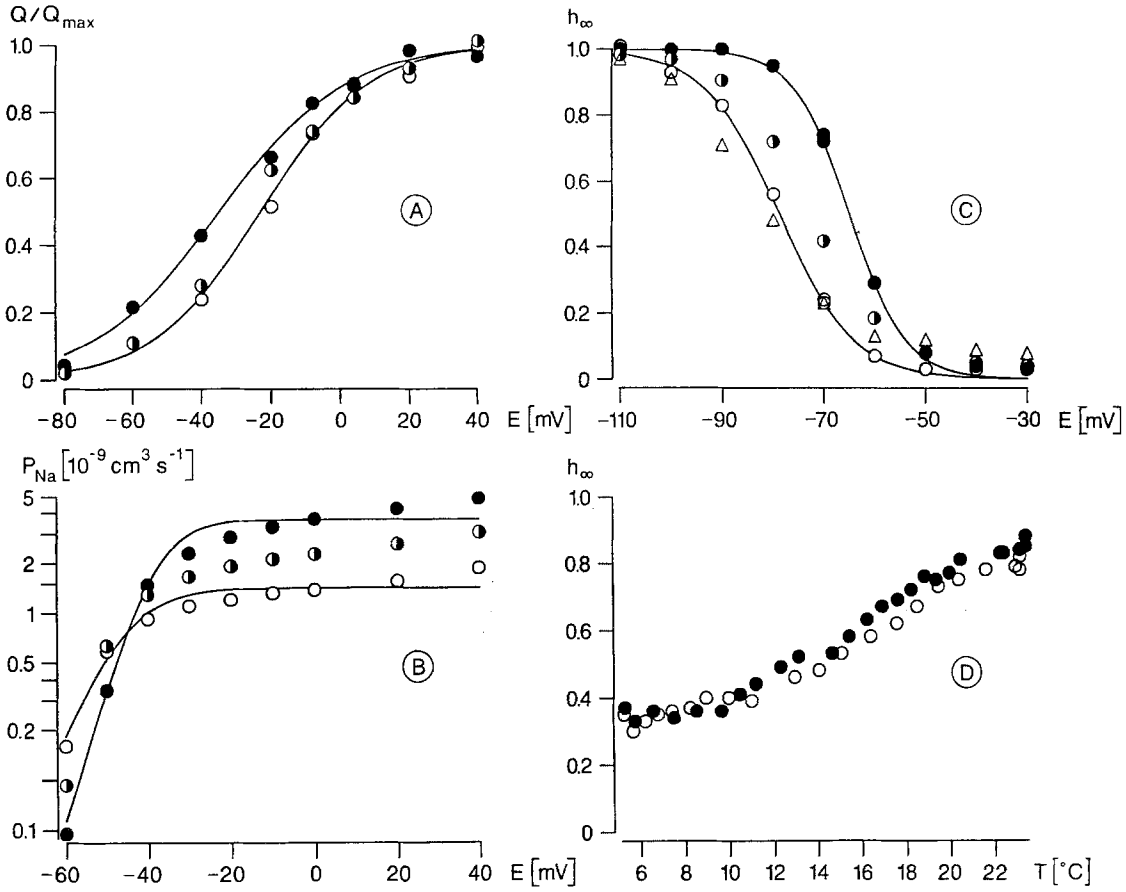


**Fig. 6.** Temperature dependence of $Q_{on}(E)$, $P_{Na}(E)$, and $h_\infty(E)$. Measurements were done in the sequence intermediate—low—intermediate—high—intermediate temperature. Data from the three measurements at intermediate temperature were averaged and displayed as one symbol (◑) for each potential value. Na currents were recorded in the presence of 5 nM TTX. (*A*) $Q_{on}(E)$ curves at 24.7°C (●), intermediate temperature (14.2, 13.9, and 13.3°C, ◑), and 6.1°C (○). $Q_{on}$ was obtained from fit of the integrated on-responses with Eq. (1), and $Q_{on}(E)$ was fitted with Eq. (3). All $Q_{on}$ values were normalized to the maximum charge ($Y_{max}$ in Eq. 3) (Expt. TE805). (*B*) $P_{Na}(E)$ curves at 24.3°C (●), intermediate temperature (12.8, 13.2, and 13.8°C, ◑), and 4.3°C (○). The $P_{Na}$ values were obtained from the peak current values according to the Goldman-Hodgkin-Katz equation (Expt. TE806). (*C*) $h_\infty(E)$ curves at 25.4°C (●), intermediate temperature (13.0, 13.3, and 13.0°C, ◑), and 4.1°C (○, △). The $h_\infty$ values at low temperature were obtained with 250-msec (○) and 50-msec (△) prepulses. All other $h_\infty$ values were obtained with 50-msec prepulses. Test pulse $E = 0$ (Expt. TE804). Continuous curves are drawn according to least squares fits of the data at low temperature (○) and high temperature (●), respectively, with Eq. (3) and correspond to the following parameters:

| | $Q_{on}(E)$ curve low/high temp. | $P_{Na}(E)$ curve low/high temp. | $h_\infty(E)$ curve low/high temp. |
|---|---|---|---|
| $E_h$(mV) | −22.5/−34.3 ± 1.8 ± 1.8 | −45.6 /−37.3 ± 2.3 ± 1.8 | −78.5/−64.6 ± 0.3 ± 0.3 |
| $\|k^*\|$ (mV) | 15.3/ 18.0 | 7.2 / 5.3 | 7.3/ 5.5 |
| $Y_{max}$ | 453 / 381 fC | 1.43/ 3.67 × $10^{-9}$ cm$^3$ sec$^{-1}$ | 1 |

(*D*) $h_\infty(E = -70$ mV) is plotted *vs.* temperature. Symbols (○) represent measurements during decrease of temperature, symbols (●) represent $h_\infty$ values obtained while increasing temperature. 50-msec prepulse, test pulse $E = 0$. (Expt. TE807)

In Figure 6*D*, $h_\infty(E = -70$ mV) is plotted *vs.* temperature for one temperature cycle. $h_\infty$ increases reversibly with increasing temperature in the range from 5 to 23°C. If the midpoint potential, $E_h$, varies linearly with temperature, $h_\infty(E = \text{const} = -70$ mV, $T$) would be expected to show the same sigmoidal shape and should be described by the same mathematical function as an $h_\infty(E, T = \text{const})$ curve, namely $h_\infty(E = -70$ mV, $T) = 1/\{1 + \exp[(T - T_h)/k^{**}]\}$. $T_h$ is the temperature where $h_\infty$ is 0.5 and $k^{**}$

is a slope factor, which characterizes the steepness of the temperature dependence of $E_h$. The general shape of $h_\infty(E = -70$ mV, $T)$ is indeed sigmoidal, but $h_\infty$ saturates at values $>0$ for $T \leq 6$°C. This deviation may be due to the fact that all $h_\infty$ values have been obtained with 50-msec prepulses, which may be insufficient at low temperature. Figure 6*C* also gives evidence that 50-msec prepulses are too short at low temperature. At low temperature, the $h_\infty(E)$ curve obtained with 250-msec prepulses is flatter than the $h_\infty(E)$ curve obtained with 50-msec prepulses, which is shown for comparison, and does not reach the abscissa for depolarizing prepulses. Thus, the present data are in accordance with the assumption that $E_h$ varies linearly with $T$.

## Discussion

The main results of the present paper are: (i) $\tau_{on}$ of the gating current and $\tau_m$ of the Na permeability are highly temperature dependent. The maximum amount of displaced charge is only weakly temperature dependent. (ii) The time constant of charge immobilization, $\tau_i$, is highly temperature dependent. The $Q_{10}$ value for $\tau_i^{-1}$ is 2.71. $\tau_i$ and the time constant of inactivation, $\tau_h$, are similar within the investigated temperature range. (iii) Temperature changes cause shifts of stationary curves $Q_{on}(E)$, $P_{Na}(E)$, and $h_\infty(E)$.

### Comparison with Previous Results

The $Q_{10}$ value of 2.54 for the time constant of the on-response of the asymmetry current reported in this paper is between the values reported by Bezanilla and Taylor (1978) and Kimura and Meves (1979) for squid axon. Bezanilla and Taylor (1978) found a $Q_{10}$ of 1.6 for early and 2.3 for late components of the on-response of the asymmetry current between 6 and 16°C. Kimura and Meves (1979) measured $Q_{10}$ values between 6.4 and 2.0 in the temperature range 0–15°C. The $Q_{10}$ given above is slightly larger than the values given in short reports of Schauf and Bullock (1979) for *Myxicola* giant axons and of Nonner et al. (1975) and Collins and Rojas (1982) for myelinated nerve. The $Q_{10}$ values of these three papers range between 2.0 and 2.4.

The weak temperature dependence of the amount of displaced charge is in accordance with the results of Bezanilla and Taylor (1978) obtained from squid axon ($Q_{10} = 1.13$ between 5 and 26°C, charge measured between $E = -100$ mV and $E = 50$ mV). Kimura and Meves (1979), however, reported considerably higher $Q_{10}$ values for $Q_{on}$ in squid axon ($Q_{10} = 1.41$ between 0 and 15°C, measured with test pulses to $E = 0$ or $E = 20$ mV). The reasons for this discrepancy may be: (i) Kimura and Meves worked in a lower temperature range and (ii) Kimura and Meves determined $Q_{on}$ with less positive pulses than Bezanilla and Taylor and I. As pointed out by Kimura and Meves (1979), shifts of the $Q_{on}(E)$ curves to the left with increasing temperature could pretend a relatively high $Q_{10}$ value for $Q_{on}(E)$ obtained with test pulses of small amplitude, although the "real" $Q_{10}$ value for $Q_{max}$ may be near one.

The present paper shows that the kinetics of charge immobilization is temperature dependent and that the time constants of charge immobilization and the time constants of fast inactivation are similar within a large temperature range. Two major arguments have been put forward in favor of the idea that charge immobilization and inactivation are more or less directly related: both have similar kinetics and potential dependence (Armstrong & Bezanilla, 1977; Nonner et al., 1978; Nonner, 1980; but *see* Meves & Vogel, 1977) and are similarly affected by neurotoxins (Nonner, 1979; but *see* Tanguy & Yeh, 1988). The similar temperature dependence of immobilization and inactivation demonstrated in the present paper is a third argument that immobilization and inactivation are strongly related, or even reflections of the same molecular process.

Shifts of $h_\infty(E)$ curves towards positive potentials with increasing temperature have been reported by Kimura and Meves (1979) for squid giant axon, by Chiu et al. (1979) for frog nodes and mammalian nodes and by Schwarz (1986) for mammalian nodes. Kimura and Meves found shifts of 7.3 mV (0 *vs.* 15°C), Chiu et al. of 5–19 mV (0 *vs.* 25°C), and Schwarz of 11.2 mV (0 *vs.* 20°C). The shift of 0.570 mV $K^{-1}$ reported above is in good agreement with the previous data, especially considering that all reports except the paper from Chiu et al. (1979) deal with different preparations.

Shifts of $P_{Na}(E)$ curves towards positive potentials with increasing temperature have been reported by some authors but were not found by others. Kimura and Meves (1979) observed shifts of 7 mV (9.2 *vs.* 15.4°C), Schwarz (1986) of 5.5 mV (0 *vs.* 20°C), whereas Chiu et al. (1979) did not find any shift ($\leq \pm 10$ mV) of $P_{Na}(E)$. The shift of 0.429 mV $K^{-1}$ reported in the present paper is close to the mean of all. The discrepancy between these findings may be at least partly due to series resistance. The influence of $R_s$ should be smaller in my experiments performed in Ri-TEA containing 5 nM TTX than in the experiments of Schwarz (1986) and Chiu et al. (1979) performed in full-Na solution without TTX. $Q_{on}(E)$ curves obtained from squid axon have been presented by Bezanilla and Taylor (1978) and by Kimura and Meves (1979). A shift of approximately 10 mV with increasing temperature (10 *vs.* 22°C) can

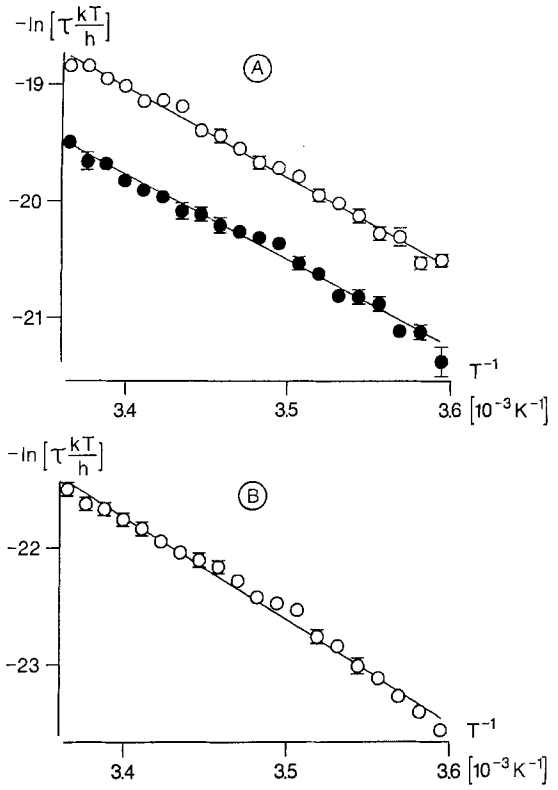


**Fig. 7.** Interpretation of the kinetic data with Eyring rate theory. $-\ln(\tau \cdot kT/h)$ was plotted *vs.* the reciprocal value of absolute temperature, $T$. The test pulse potential is the same ($E$ = 4 mV) for all measurements. (*A*) $\tau = \tau_m$ (○), $\tau = \tau_{on}$ (●). (*B*) $\tau = \tau_h$. The straight lines are drawn according to the results of linear regression yielding the following apparent values of activation enthalpy $\Delta H_a$ and activation entropy $\Delta S_a$:

| | $\Delta H_a$ (kJ mol$^{-1}$) | $\Delta S_a$ (J mol$^{-1}$ K$^{-1}$) | mean $Q_{10}$ ± SEM |
|---|---|---|---|
| $\tau_{on}$ | 61.3 | 44.0 | 2.54 ± 0.07 |
| $\tau_m$ | 64.2 | 60.2 | 2.64 ± 0.06 |
| $\tau_h$ | 73.1 | 67.8 | 3.00 ± 0.09 |

The $Q_{10}$ values shown in the table were calculated from $\ln(\tau)$ *versus* $T$ plots. The Figure contains data from 394 Na current records (5 experiments) and 99 gating current records (7 experiments)

be seen in Fig. 1*B* of Bezanilla and Taylor (1978), but was not further discussed by the authors. Kimura and Meves could not decide whether the high $Q_{10}$ for $Q_{on}$ they observed was due to an increase of $Q_{max}$ or due to a shift of the $Q_{on}(E)$ curve towards negative potentials. This uncertainty arises from the fact that—as can be seen in their Fig. 9—the saturation of charge at high positive potentials is not pronounced.

It is surprising that $Q_{on}(E)$ curves are shifted to the left, whereas $P_{Na}(E)$ curves are shifted to the right when temperature is increased. A similar observation has been reported by Conti et al. (1982, 1984), who found that increasing pressure shifts $P_{Na}(E)$ towards positive potentials, but does not shift $Q_{on}(E)$. The results of the present paper and the findings of Conti et al. (1982, 1984) can be explained with the hypothesis that transitions between the closed states of the Na channel contribute far more to the total charge movement than the final step preceding the opening of the Na channel. Indeed, there is a lot of evidence in favor of this hypothesis. The Na channel models of Armstrong and Gilly (1979) and Horn and Vandenberg (1984) assume this final step to be rate limiting; consequently, the corresponding component of gating current may have been lost in the baseline. Other models even postulate that this step is electrically silent (Edmonds, 1987). Therefore, the assumption that the final step makes negligible contribution to gating current seems to be justified and will be also made in the following model.

## Thermodynamic Interpretation of the Kinetic Data and the Shifts

The interpretation of the present results is complicated by the fact that there is no universal model of Na channel gating. It is controversal how many states exist, how they are linked by reaction steps, and which steps are slow and which are fast.

If one accepts that the time constant of gating current and the time constants of activation and inactivation of Na current each reflect mainly one reaction step, their temperature dependence may be explained in terms of Eyring rate theory. For a chemical reaction with a single energy barrier, rate constant $r$, standard activation enthalpy $\Delta H_a$, and standard activation entropy $\Delta S_a$ are related as follows (*see* Tsien & Noble, 1969; Marshall, 1978):

$$-\ln(1/r \cdot kT/h) = -\Delta H_a/RT + \Delta S_a/R. \quad (5)$$

$k$ is the Boltzmann constant, $h$ the Planck constant, $R$ the gas constant, and $T$ the absolute temperature. If the backward rate constants are much smaller than forward rate constants (this should be the case at $E$ = 4 mV), one may substitute $1/r$ by the relaxation time constant $\tau$. Figure 7 shows a plot of $-\ln(\tau \cdot kT/h)$ *versus* $1/T$ for $\tau_{on}$, $\tau_m$, and $\tau_h$. All relations can be satisfactorily fitted with straight lines in the temperature range from 5 to 24°C. The values of $\Delta H_a$ and $\Delta S_a$ obtained from these plots (*see* legend of Fig. 7) are apparent values, because one does not exactly know how many reaction steps contribute to the observed relaxation time constant and how many energy barriers are crossed. Nevertheless, it

is interesting to compare these apparent activation entropy values with the values of Tsien and Noble (1969), which were calculated from the $Q_{10}$ values of Frankenhaeuser and Moore (1963). The data of the present paper indicate that the apparent activation entropy values $\Delta S_a$ obtained from $\tau_{on}$, $\tau_m$, and $\tau_h$ are positive (*see* legend of Fig. 7). Tsien and Noble (1969) report a similar $\Delta S_a$ value for the inactivation process, but a completely different, i.e., negative, value for the activation process. The reason for this discrepancy is the low temperature dependence of $\tau_m$ in the data set of Frankenhaeuser and Moore (1963, $Q_{10} = 1.84$ for $\alpha_m$).

The temperature dependent shifts of $Q_{on}$, $P_{Na}$, and the fraction of inactivated channels ($1\text{-}h_\infty$) which are assumed to be steady-state parameters and are symbolized as $x_\infty$, can be explained as follows: assuming two-state gating mechanism $A \leftrightarrow B$, the electrochemical equilibrium between these two states can be described by the function

$$x_\infty(E) = 1/\{1 + \exp[(\Delta G - z \cdot F \cdot E)/RT]\} \qquad (6)$$

where $x_\infty(E)$ is the fraction of "gates" in state $B$, $\Delta G = G_B - G_A$ (which are the standard free energy values of $B$ and $A$ in the absence of electric field) and $z$ is the number of elementary charges associated with the transition $A \rightarrow B$ (*see* Marshall, 1978). With $\Delta G = \Delta H - T \cdot \Delta S$, where $\Delta H$ and $\Delta S$ denote standard enthalpy and entropy differences, respectively, the midpoint potential $E_h$ of the curve (where $x_\infty = 0.5$) can be calculated as

$$E_h = -T \cdot \Delta S/zF + \Delta H/zF. \qquad (7)$$

Temperature dependence of $E_h$ is obvious if $\Delta S$ is different from 0. Finally, one may calculate $\Delta S = -zF \cdot \Delta E_h/\Delta T$; this approach, however, is strictly valid only if $\Delta H$ and $\Delta S$ are independent of temperature. A variation of $\Delta H$ and $\Delta S$ with temperature, which has been reported for lysozyme (Pfeil & Privalov, 1976), would predict a change of $dE_h/dT$ with temperature. No such change, however, was found experimentally: $Q_{on}(E)$, $P_{Na}(E)$, and $h_\infty(E)$ curves at intermediate temperature are approximately in the middle between the curves at high and low temperature. The shape of $h_\infty(E = -70\text{ mV}, T)$ in Fig. 6*D* is also in accordance with a constant $dE_h/dT$, as mentioned above. Thus, $\Delta H$ and $\Delta S$ of the Na channel protein seem to be, in first approximation, constant within the investigated temperature range.

If one assumes that the final step opening the Na channel makes only little contribution to the gating current (*see* above), an entropy profile of Na channel gating can now be deduced from the observed shift values. Such a hypothetical entropy *vs.* state diagram, based on a Markovian model with four closed states, is given in Fig. 8; details of the calculation procedure are described in the legend of the figure.

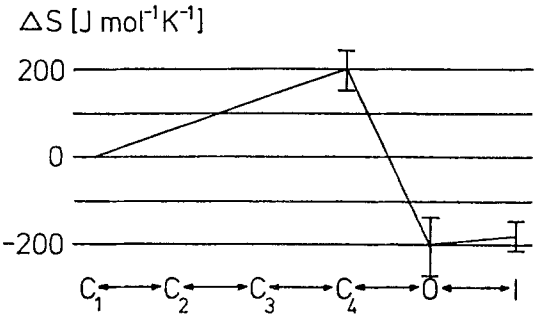


**Fig. 8.** Interpretation of the equilibrium data: A hypothetical entropy profile of Na channel. Entropy value $\Delta S$ of a certain state relative to $C_1$ was calculated from the mean shifts, the mean slope factors, and the mean temperatures in Table 2 according to Eq. (7). Handling the shifts of $Q_{on}(E)$ and $h_\infty(E)$ is straightforward, because the experimental data are fitted conveniently with Eq. (6). From the shift of the $Q_{on}(E)$ curve, the average $\Delta S$ for a transition $C_i \rightarrow C_{i+1}$ can be calculated as $\Delta S = -zF\,\Delta E_h/\Delta T = 66$ J mol$^{-1}$ K$^{-1}$. From the shift of the $h_\infty(E)$ curve, $\Delta S$ for the transition $C_1 \rightarrow I$ can be calculated as $-182$ J mol$^{-1}$ K$^{-1}$. Treatment of the shift of the $P_{Na}(E)$ curve is more difficult, because $P_{Na}(E)$ curves are not conveniently fitted with Eq. (6). The curve is asymmetric and contains information about the step $C_4 \rightarrow 0$ towards positive potentials and about the transitions $C_1 \rightarrow \rightarrow 0$ towards negative potentials (Almers, 1978). Shifts and steepness factors were obtained from fits in $\ln(P_{Na})$ *versus* $E$ plots, which should weight the data in the negative potential range relatively high and therefore describe the $C_1 \rightarrow \rightarrow 0$ transitions; the corresponding $\Delta S$ is calculated as $-201$ J mol$^{-1}$ K$^{-1}$. The assumption of four closed states, i.e., four reaction steps before the open state is reached is based on the observation that $k^*$ for $Q_{on}(E)$ is 3.6 times as large as for $P_{Na}(E)$, but is somewhat arbitrary. It is assumed that each of the three reaction steps between the closed states leads to the same change of entropy $\Delta S$. Bypass reactions, which could, for example, lead from $C_4$ directly to $I$ (Horn & Vandenberg, 1984), are not displayed. They should, however, have no consequences for the estimation of the entropy profile, because introducing a bypass reaction does not change the equilibrium if the system still obeys microscopic reversibility

Different interpretations of the shifts induced by temperature changes are, however, possible.

i) Screening of surface charges on the outer side of the membrane may depend on temperature, because the equation of Grahame (1947) includes absolute temperature $T$ as well as the dielectric constant of water, which is itself a function of $T$ (Lax, 1967). The shifts of potential-dependent parameters calculated from Grahame's equation using the surface charge density of Vogel (1974) are, however, by a factor of about two smaller than the observed shifts. Furthermore, the screening hypothesis can

hardly explain why increasing temperature shifts $Q_{on}$, on one hand, and $P_{Na}$ and $h_\infty$, on the other hand, into different directions.

ii) A phase transition of the membrane lipids could occur, which might change the equilibrium of reactions of the Na channel. This seems unlikely, since the shifts are observed within the whole investigated temperature range 5–25°C, whereas transition temperatures are below 10°C in frog nerve (Schwarz, 1979).

iii) Decreasing temperature may select a population of channels with steady-state properties different from the average. Matteson and Armstrong (1982) postulated "sleepy" channels at low temperature (1°C) in squid axon. They found, however, similar $P_{Na}(E)$ characteristics for "sleepy" channels and normal channels. As the amount of gating charge is constant within the investigated temperature range (Fig. 1*D*), "sleepy" channels—if existing in the node of Ranvier at about 6°C—may have a "nonsleepy" gating machinery.

## Consequences for Models of Na Channel Gating

Figure 8 shows that considerable entropy changes may occur when a Na channel passes from closed through open to inactivated states. Howarth (1975) observed measurable heat production during an action potential and explained this phenomenon with large entropy changes of the membrane, too. Baumann (1978) reported $\Delta S_a$ and $\Delta S$ values in the same order of magnitude for the conversion between metarhodopsin I and II ($\Delta S_a$ = 230 J mol$^{-1}$ $K^{-1}$ and $\Delta S$ = 142 J mol$^{-1}$ $K^{-1}$). Considering the lower molecular weight of metarhodopsin, the entropy changes seem to be even larger in this molecule. Entropy is a measure of the disorder of a system, e.g., the Na channel including its lipid and aqueous environment. Figure 8 therefore suggests that the intermediate closed states of the Na channel are states of low order, whereas the open and the inactivated state are states of high order. The protein structure may initially unfold and then collapse. It would be interesting to test whether recent hypotheses concerning the molecular mechanisms of Na channel gating are in accordance with the entropy profile given in the present paper.

I especially want to thank Prof. W. Vogel for his continuous support and many stimulating discussions during all stages of the work. I thank Prof. H. Meves, Prof. B. Neumcke, and Dr. D. Siemen for critically reading the manuscript and Elke Schmidt for her perfect technical assistance. Financial support from the Deutsche Forschungsgemeinschaft (Vo 188/12-6) is gratefully acknowledged.

## References

Almers, W. 1978. Gating currents and charge movements in excitable membranes. *Rev. Physiol. Biochem. Pharmacol.* **82:**96–190

Armstrong, C.M., Bezanilla, F. 1973. Currents related to movement of the gating particles of the sodium channels. *Nature (London)* **242:**459–461

Armstrong, C.M., Bezanilla, F. 1977. Inactivation of the sodium channel. II. Gating current experiments. *J. Gen. Physiol.* **70:**567–590

Armstrong, C.M., Gilly, W.F. 1979. Fast and slow steps in the activation of sodium channels. *J. Gen. Physiol.* **74:**691–711

Baumann, C. 1978. The equilibrium between metarhodopsin I and metarhodopsin II in the isolated frog retina. *J. Physiol. (London)* **279:**71–80

Bezanilla, F., Taylor, R.E. 1978. Temperature effects on gating currents in the squid giant axon. *Biophys. J.* **23:**479–484

Chiu, S.Y., Mrose, H.E., Ritchie, J.M. 1979. Anomalous temperature dependence of the sodium conductance in rabbit nerve compared with frog nerve. *Nature (London)* **279:**327–328

Collins, C.A., Rojas, E. 1982. Temperature dependence of the sodium channel gating kinetics in the node of Ranvier. *Q. J. Expt. Physiol.* **67:**41–55

Conti, F., Fioravanti, R., Segal, J.R., Stühmer, W. 1982. Pressure dependence of the sodium currents of squid giant axon. *J. Membrane Biol.* **69:**23–34

Conti, F., Inoue, I., Kukita, F., Stühmer, W. 1984. Pressure dependence of sodium gating currents in the squid giant axon. *Eur. Biophys. J.* **11:**137–147

de Haas, V. 1987. Personal computers for stimulus generation, data acquisition and analysis in electrophysiological experiments. *Pfluegers Arch.* **408:**R85

Drouin, H., Neumcke, B. 1974. Specific and unspecific charges at the sodium channels of the nerve membrane. *Pfluegers Arch.* **351:**207–229

Dubois, J.M., Schneider, M.F. 1982. Kinetics of intramembrane charge movement and sodium current in frog node of Ranvier. *J. Gen. Physiol.* **79:**571–602

Dudel, J., Rüdel, R. 1970. Voltage and time dependence of excitatory sodium current in cooled sheep Purkinje fibres. *Pfluegers Arch.* **315:**136–158

Edmonds, D.T. 1987. A comparison of sodium channel kinetics in the squid axon, the frog node and the frog node with BTX using the "silent gate" model. *Eur. Biophys. J.* **15:**27–33

Frankenhaeuser, B., Moore, L.E. 1963. The effect of temperature on the sodium and potassium permeability changes in myelinated nerve fibres of *Xenopus laevis*. *J. Physiol. (London)* **169:**431–437

Grahame, D.C. 1947. The electrical double layer and the theory of electrocapillarity. *Chem. Rev.* **41:**441–501

Horn, R., Vandenberg, C.A. 1984. Statistical properties of single sodium channels. *J. Gen. Physiol.* **84:**505–534

Howarth, J.V. 1975. Heat production in non-myelinated nerves. *Phil. Trans. R. Soc. London B* **270:**425–432

Jennrich, R.I., Ralston, M.L. 1979. Fitting nonlinear models to data. *Annu. Rev. Biophys. Bioeng.* **8:**195–238

Jonas, P., Vogel, W. 1988. Temperature dependence of asymmetry currents in peripheral nerve. *Pfluegers Arch.* **411:**R162

Kimura, J.E., Meves, H. 1979. The effect of temperature on the asymmetrical charge movement in squid giant axons. *J. Physiol. (London)* **289:**479–500

Kniffki, K.-D., Siemen, D., Vogel, W. 1981. Development of sodium permeability inactivation in nodal membranes. *J. Physiol. (London)* **313:**37–48

Lax, E. (editor) 1967. Taschenbuch für Chemiker und Physiker. Band I. Makroskopische physikalisch-chemische Eigenschaften. p. 627. Springer, Berlin

Marshall, A.G. 1978. Biophysical Chemistry. Principles, Techniques, and Applications. Wiley, New York

Matteson, D.R., Armstrong, C.M. 1982. Evidence for a population of sleepy sodium channels in squid axon at low temperature. *J. Gen. Physiol.* **79:**739–758

Meves, H., Vogel, W. 1977. Inactivation of the asymmetrical displacement current in giant axons of *Loligo forbesi*. *J. Physiol. (London)* **267:**377–393

Neumcke, B., Nonner, W., Stämpfli, R. 1976. Asymmetrical displacement current and its relation with the activation of sodium current in the membrane of frog myelinated nerve. *Pfluegers Arch.* **363:**193–203

Nonner, W. 1969. A new voltage clamp method for Ranvier nodes. *Pfluegers Arch.* **309:**176–192

Nonner, W. 1979. Effects of *Leiurus* scorpion venom on the "gating" current in myelinated nerve. *Adv. Cytopharmacol.* **3:**345–352

Nonner, W. 1980. Relations between the inactivation of sodium channels and the immobilization of gating charge in frog myelinated nerve. *J. Physiol. (London)* **299:**573–603

Nonner, W., Rojas, E., Stämpfli, R. 1975. Displacement currents in the node of Ranvier. Voltage and time dependence. *Pfluegers Arch.* **354:**1–18

Nonner, W., Rojas, E., Stämpfli, R. 1978. Asymmetrical displacement currents in the membrane of frog myelinated nerve: Early time course and effects of membrane potential. *Pfluegers Arch.* **375:**75–85

Pfeil, W., Privalov, P.L. 1976. Thermodynamic investigations of proteins. III. Thermodynamic description of lysozyme. *Biophys. Chem.* **4:**41–50

Sachs, L. 1984. Angewandte Statistik. Anwendung statistischer Methoden. p. 330. Springer, Berlin

Schauf, C.L., Bullock, J.O. 1979. Modifications of sodium channel gating in *Myxicola* giant axons by deuterium oxide, temperature, and internal cations. *Biophys. J.* **27:**193–208

Schwarz, J.R. 1986. The effect of temperature on Na currents in rat myelinated nerve fibres. *Pfluegers Arch.* **406:**397–404

Schwarz, W. 1979. Temperature experiments on nerve and muscle membranes of frogs. Indications for a phase transition. *Pfluegers Arch.* **382:**27–34

Tanguy, J., Yeh, J.Z. 1988. Batrachotoxin uncouples gating charge immobilization from fast Na inactivation in squid giant axons. *Biophys. J.* **54:**719–730

Tsien, R.W., Noble, D. 1969. A transition state theory approach to the kinetics of conductance changes in excitable membranes. *J. Membrane Biol.* **1:**248–273

Vogel, W. 1974. Calcium and lanthanum effects at the nodal membrane. *Pfluegers Arch.* **350:**25–39

Received 1 March 1989; revised 29 June 1989